ELSEVIER

International Journal of Mass Spectrometry 181 (1998) 59–66

International Journal of Mass Spectrometry

Vacuum ultraviolet photoionization and photodissociation of ferrocene

S.-J. Han[a], M.C. Yang[a], C.H. Hwang[a], D.H. Woo[a], J.R. Hahn[a], H. Kang[a,*], Y. Chung[b]

[a]*Department of Chemistry and* [b]*Pohang Accelerator Laboratory, Pohang University of Science and Technology, Pohang, Gyeongbuk 790-784, South Korea*

Received 23 March 1998; accepted 28 August 1998

Abstract

Photoionization and photodissociation of ferrocene [$Fe(C_5H_5)_2$] is examined by using vacuum ultraviolet (VUV) photons from a synchrotron radiation source and a time-of-flight (TOF) photoionization mass spectrometer. VUV absorption by ferrocene results in $Fe(C_5H_5)_2^{\cdot+}$, $FeC_5H_5^+$, $FeC_3H_3^+$, $Fe^{\cdot+}$ and $C_{10}H_x^{\cdot+}$ ($x = 8 - 10$). The dependency of the product distribution on photon energy indicates sequential elimination of $C_5H_5\cdot$ ligands as a major dissociation channel, but concerted elimination of two $C_5H_5\cdot$ ligands also takes place to a lesser degree. Through analysis of TOF peak shape, it is found that $Fe(C_5H_5)_2^{\cdot+}$ molecular ion dissociates into $FeC_5H_5^+$ and $C_5H_5\cdot$ via two channels. One is nonstatistical dissociation with a fast rate, and the other is slow unimolecular decay that becomes more discernible at low photon energy. The rate of unimolecular decay, exemplified by a value of $k = 2.4 \pm 1.0 \times 10^6\ s^{-1}$ at photon energy of 14.76 eV, is well in accord with the RRKM rate. (Int J Mass Spectrom 181 (1998) 59–66) © 1998 Elsevier Science B.V.

Keywords: Ferrocene; Photoionization; Photodissociation; Vacuum ultraviolet; Synchrotron radiation

1. Introduction

Along with the increasing availability of modern synchrotron radiation facilities and the development of vacuum ultraviolet (VUV) laser technology, the number of studies of VUV spectroscopy and photochemistry has grown remarkably in the recent years [1,2]. An interesting branch of VUV photochemistry is photoionization and photodissociation of large polyatomic molecules. Upon VUV absorption, polyatomic molecules often give rise to rich, if not too complex, fragmentation patterns that are closely related to the chemical nature of the molecules. Various experimental techniques have been employed to investigate ionization and dissociation processes of polyatomic molecules in the VUV regime [1–3].

Ferrocene [bis(cyclopentadienyl)iron(II); $Fe(C_5H_5)_2$ or $FeCp_2$, where Cp· represents a cyclopentadienyl radical] is an organometallic sandwich compound, and its molecular structure has been reported in detail [4,5]. Ferrocene has a high density of electronic states of various multiplicities [6,7] and a large number of vibrational modes [8–10]. In this regard, it might be considered that ferrocene in the gas phase would undergo dissociation via statistical channels, and it

* Corresponding author.

PII S1387-3806(98)14176-3

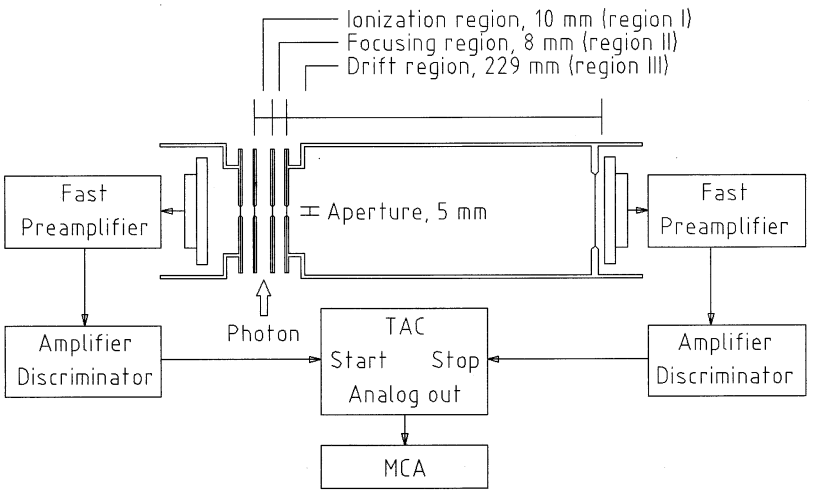

Fig. 1. Schematic diagram of the instrumental configuration for VUV photoionization/photodissociation experiment using TOF detection.

does so under many circumstances [11–13]. However, experimental observations have also been made that show inconsistency with the statistical dissociation [11,12]. Such reports are interesting because non-statistical photodissociation is very rare among large organic polyatomic ions [14]. Ionization and dissociation of ferrocene has been investigated by using various excitation methods, including UV multiphoton absorption [11–13,15–18], VUV absorption [19] and electron impact [17,18,20]. UV multiphotons dissociate ferrocene molecules predominantly to metal atoms, followed by photoionization of the metal atoms [11,15]. Time-of-flight (TOF) photoelectron spectra of ferrocene were examined [16], probing wavelength-dependency of the $Fe^{\cdot+}$ production by multiphoton ionization and dissociation (MPI/MPD). Later, the competition between the ligand dissociation reaction and the molecular ionization was reported [17,18] from a wavelength-dependent MPI/MPD study. Photoionization study with VUV light [19] provided the appearance potentials for molecular and fragmented ions of ferrocene. Dissociation of $FeCp_2^{\cdot+}$ ion has also been investigated by time-resolved photodissociation study [13] and by hyperthermal ion beam collision with a solid surface, or surface-induced dissociation (SID) [21,22]. In VUV regime, the photoionization and fragmentation mechanism of ferrocene is still not clearly established. In this work, we explore VUV-induced reactions of ferrocene by using synchrotron radiation in conjunction with a TOF photoionization mass spectrometer based on a coincident electron and ion detection method.

2. Experimental

The experiment was performed at the 2B2 synchrotron beamline of Pohang Light Source (PLS). The beamline provides monochromatized photon beams in the range of 5–35 eV by using a 3 m normal incidence monochromator. The schematic diagram of the TOF photoionization mass spectrometer is shown in Fig. 1. The mass spectrometer consists of an ionization region (region I), a space focusing and acceleration region (region II), and a field-free drift region (region III). The photoelectrons and the photoions simultaneously produced in region I were accelerated in the opposite directions and detected by microchannel plates (MCPs). MCPs of a large diameter (40 mm) were used in order to reduce the discrimination effect of a detector against the energetic ions that were ejected perpendicular to the direction of an ion extraction field. The coincident electron and ion signals were fed into “start” and “stop” inputs of a time-to-amplitude convertor (TAC), respectively. TAC produced an analog pulse with its height proportional to

the ion flight time, or equivalently, to the square root of the ion mass. The ion mass spectrum was obtained by analyzing the pulse heights with a multichannel analyzer. The kinetic energy of the photoelectrons was not analyzed.

The ferrocene vapor was introduced into the ionization region through a short, direct inlet tube made of stainless steel. The holder of ferrocene powder samples and the inlet tube were heated to a controlled temperature so that the ferrocene vapor pressure in the ionization region reached 5×10^{-6} Torr. Under this condition, the pressure in the drift region was maintained at 1×10^{-8} Torr.

3. Results and discussion

3.1. The products of VUV photoionization and photodissociation

Upon VUV irradiation, $FeCp_2$ molecules undergo ionization and dissociation reactions. These processes occur by absorption of single photon under the given condition of photon beam flux. The reaction patterns are exemplified by the TOF mass spectra of Fig. 2, showing the product ion intensities at three different incident photon energies (14.76, 16.53 and 22.55 eV). The major product ions are identified as ferrocene molecular ion ($FeCp_2^{\cdot+}$, m/z = 186 u) and the dissociation products resulting from Cp· ligand elimination ($FeCp^+$ and $Fe^{\cdot+}$ at m/z = 121 and 56 u, respectively). At high photon energy, $FeC_3H_3^+$ (m/z = 95 u) and $C_{10}H_{10}^{\cdot+}$ ions (m/z = 130 u) are also produced in small but meaningful populations. The peak labeled as $C_{10}H_{10}^{\cdot+}$ may also contain $C_{10}H_8^{\cdot+}$ (m/z = 128 u) because mass resolution of the TOF instrument is about 2 u.

The branching ratio into the various product ions is examined as a function of incident photon energy, and the result is shown in Fig. 3 for the photon energy range of 14–33 eV. It is clear that the degree of molecular fragmentation increases with increasing photon energy. Nonetheless, the molecular ion is the mostly dominant product even at high photon energy. In the low energy region, the threshold energy for

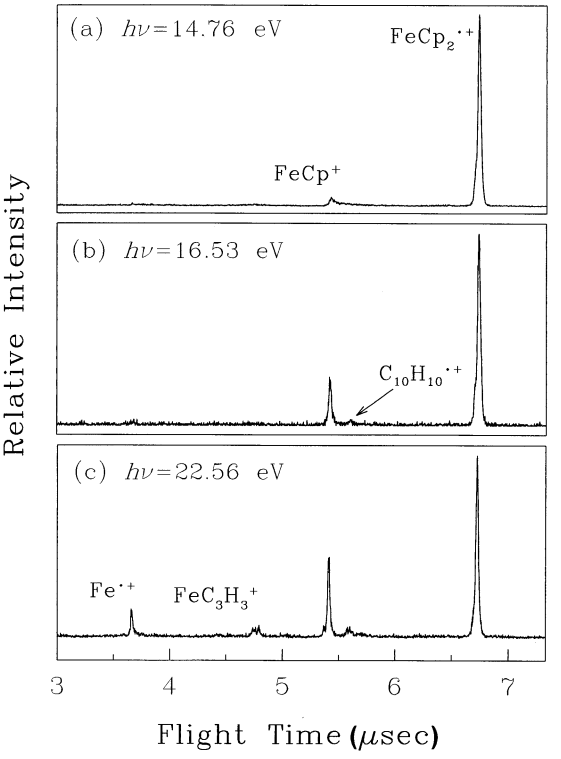

Fig. 2. TOF mass spectra of the positive ions generated by photoionization and photodissociation of ferrocene. The employed photon energies are 14.76 eV (a), 16.53 eV (b) and 22.55 eV (c).

$FeCp^+$ production is observed at 14 eV. The yield for $Fe^{\cdot+}$ production is almost zero at this energy, but increases substantially from about 18 eV. The difference of 4 eV between the threshold energies for $FeCp^+$ and Fe^+ is approximately equal to the second Cp dissociation energy (Table 1), an indication that $Fe^{\cdot+}$ formation occurs via consecutive dissociation processes of two ligands [reaction (1)]

$$Fe(C_5H_5)_2 + h\nu \rightarrow [Fe(C_5H_5)^+]^* + C_5H_5\cdot + e^- \rightarrow Fe^{\cdot+} + 2C_5H_5\cdot + e^- \quad (1)$$

The threshold energies may contain a substantial kinetic shift because of fast ion extraction ($\leq$1 μs) in the present experiment, but its contribution can largely be canceled out by taking the difference between the two threshold energies. The threshold energy measurement has also been reported by Bär et al.

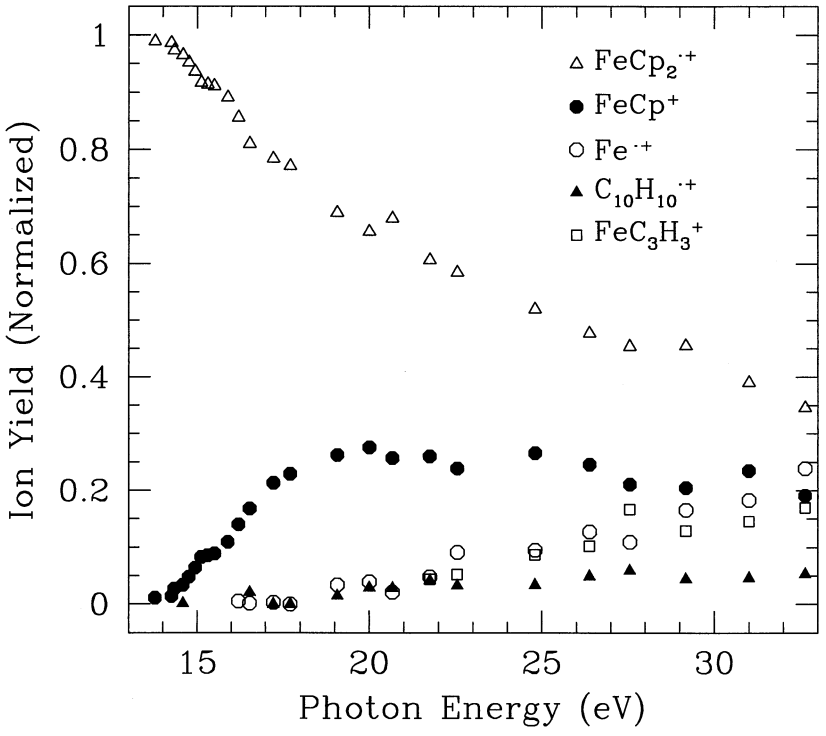

Fig. 3. The yield of various product ions as a function of incident photon energy for the range of 14–33 eV.

[19] for the production of $FeCp_2^{\cdot+}$, $FeCp^+$, and $Fe^{\cdot+}$ ions from $FeCp_2$. Their work showed a small intensity of $Fe^{\cdot+}$ ion even below photon energy of 18 eV, persisting down to 13.5 eV. Such Fe^+ production at the low energy cannot be discerned from a noise level in Fig. 3 because of low detection sensitivity of our instrument. This low energy channel was attributed [19] to concerted elimination of two Cp ligands [reaction (2a)].

$$Fe(C_5H_5)_2 + h\nu \rightarrow [Fe(C_5H_5)_2^{\cdot+}]^* + e^- \rightarrow Fe^{\cdot+} + C_{10}H_{10} + e^- \quad (2a)$$

$$\rightarrow Fe + C_{10}H_{10}^{\cdot+} + e^- \quad (2b)$$

It may be possible that the concerted transition state for reaction (2a) branches also into $C_{10}H_{10}^{\cdot+}$ production [reaction (2b)] because the ionization energies of Fe and $C_{10}H_{10}$ are not much different (Table 1). Further dissociation of $C_{10}H_{10}^{\cdot+}$ can produce $C_{10}H_8^{\cdot+}$ by H_2 elimination [22]. $C_{10}H_x^{\cdot+}$ ($x = 8 - 10$) ions are indeed observed in small intensity (Fig. 2), providing evidence for occurrence of the concerted reactions.

The present result by VUV single photon absorption can be compared with the $FeCp_2$ activation

Table 1
Literature thermochemical data related to $Fe(C_5H_5)_2$ ionization and dissociation

Reaction	Energy (eV)
$Fe(C_5H_5)_2 \rightarrow Fe(C_5H_5)_2^{\cdot+} + e^-$	6.75[a], 6.99[b]
$Fe(C_5H_5)_2 \rightarrow Fe(C_5H_5)^+ + C_5H_5\cdot + e^-$	13.16[a], 11.6[b]
$Fe(C_5H_5)_2 \rightarrow Fe^{\cdot+} + 2\ C_5H_5\cdot + e^-$	16.8[a], 15.6[b]
$Fe(C_5H_5)_2 \rightarrow Fe^{\cdot+} + C_{10}H_{10} + e^-$	13.5[a]
$Fe(C_5H_5)_2 \rightarrow Fe + C_{10}H_{10}^{\cdot+} + e^-$	13.8[c]
$Fe(C_5H_5)_2^{\cdot+} \rightarrow Fe(C_5H_5)^+ + C_5H_5\cdot$	6.41[a], 4.61[b], 3.7[d]
$Fe(C_5H_5)^+ \rightarrow Fe^{\cdot+} + C_5H_5\cdot$	3.64[a], 4.0[b], 4.3[d]
$Fe(C_5H_5)_2^{\cdot+} \rightarrow Fe^{\cdot+} + 2C_5H_5\cdot$	10.1[a], 8.6[b], 8.0[d]

[a] Photoionization study: [19].
[b] Electron impact study: [18].
[c] Electron impact study: [20].
[d] Time-resolved photodissociation study of $FeCp_2^{\cdot+}$ ion: [13].

results by other means. UV MPI/MPD of ferrocene resulted in exclusive molecular dissociation, prior to ionization of an Fe atom for photon wavelengths of 380–390 and 445–453 nm [11,15,16]. MPI/MPD at higher photon energies (193 and 248 nm) produced $FeCp_2^{\cdot+}$, $FeCp^+$ and $Fe^{\cdot+}$ [17,18]. $C_{10}H_{10}^{\cdot+}$ was not observed in these MPI/MPD works. The present VUV fragmentation result is similar to the electron impact results [17,20], in that $FeC_3H_3^+$ and $C_{10}H_{10}^{\cdot+}$ are produced as additional products. The $C_{10}H_{10}^{\cdot+}$ elimination [reaction (2b)], being a concerted reaction, is energetically more favorable than the sequential ligand elimination processes [reaction (1)], but should be more demanding entropically because the necessity of Cp-Cp association. The sequential ligand dissociation is known [16–18] to occur very fast, for example, within 10 ns under a UV MPI/MPD condition that gives molecular internal energy comparable to single VUV photon absorption. The concerted elimination reaction, on the other hand, is expected to occur much more slowly because of an entropy barrier. In the present experiment, the two reactions of very different speeds take place simultaneously. These seemingly contradictory observations can be explained if one assumes that the concerted reaction takes place on the electronic excited potential surfaces of long lifetimes. There are numerous electronic states of ferrocene [6,7] that can be populated by either VUV photon absorption or electron impact. SID is a unique kind of method that can excite molecular ions to an energy comparable to VUV absorption. SID of $FeCp_{10}^{\cdot+}$ at hyperthermal collision energy produces $FeCp_2^{\cdot+}$, $FeCp^+$, $FeC_3H_3^+$, $Fe^{\cdot+}$ and $C_{10}H_8^{\cdot+}$ [21,22]. For the case of SID, the yield for molecular reflection ($FeCp_2^{\cdot+}$) drastically decreases at high collision energy (>30 eV), to a value much smaller than the fragmented ion yields. In comparison, the $FeCp_2^{\cdot+}$ yield in Fig. 3 continues to be the largest even at high photon energies.

3.2. TOF peak shape and dissociation dynamics

The fragmentation peaks in a TOF spectrum correspond to the ions rapidly dissociated inside the ionization region (region I in Fig. 1) upon VUV absorption. The fragmented ions of different masses acquire different velocities during the electrostatic acceleration, and are distinguished in a TOF spectrum. When parent ions dissociate at a much delayed time and thus in the field-free drift region (region III), the daughter ions have the same velocity as the parent ions. In this case the two ions appear within the envelope of a single TOF peak. If dissociation occurs while parent ions pass through the acceleration and focusing region (region II), then the daughter ions give rise to an asymmetric tail in the TOF peak [23]. The duration for parent $FeCp_2^{\cdot+}$ ions to stay inside region II is of the order of 1 μs or less in the present experiment, with the extraction voltage of region II controlled between 0.5–3 kV across a distance of 8 mm. Accordingly, the dissociation rate of a comparable timescale can be measured by analyzing a TOF peak shape.

Fig. 4 exemplifies an asymmetric TOF peak with a low velocity tail observed for fragmented ions, showing the $FeCp^+$ ion signals produced at photon energy of 14.76 eV (84 nm). Most of the daughter ions exhibit such an asymmetric TOF distribution, when they are produced by low energy photons. In order to analyze the peak shape of Fig. 4, a convolution fit is employed using the Lorentzian function with a single exponential decay in the form,

$$S(t) = \sum_{t=t_0}^{t_f} \frac{Ae^{-kt^*}}{1 + B(t' - t)^2}, \tag{3}$$

where $S(t)$ represents the intensity profile of fragment ions (the TOF distribution), and t is the TOF of an ion to a detector. The Lorentzian function is used to describe the inherent feature of a TOF signal, accounting for the TOF broadening because the thermal motions, the instrumental resolution and the kinetic energy released during molecule dissociation. The Lorentzian parameter B is determined from a peak shape without a tail that appears at sufficiently high photon energy. If parent ions dissociate in region II of high potential gradient, the emanating daughter ions will acquire various degrees of electrostatic acceleration depending on the position, and thus the time, of their birth. That is, the dispersion in the time of birth gives rise to asymmetric broadening in the TOF peak

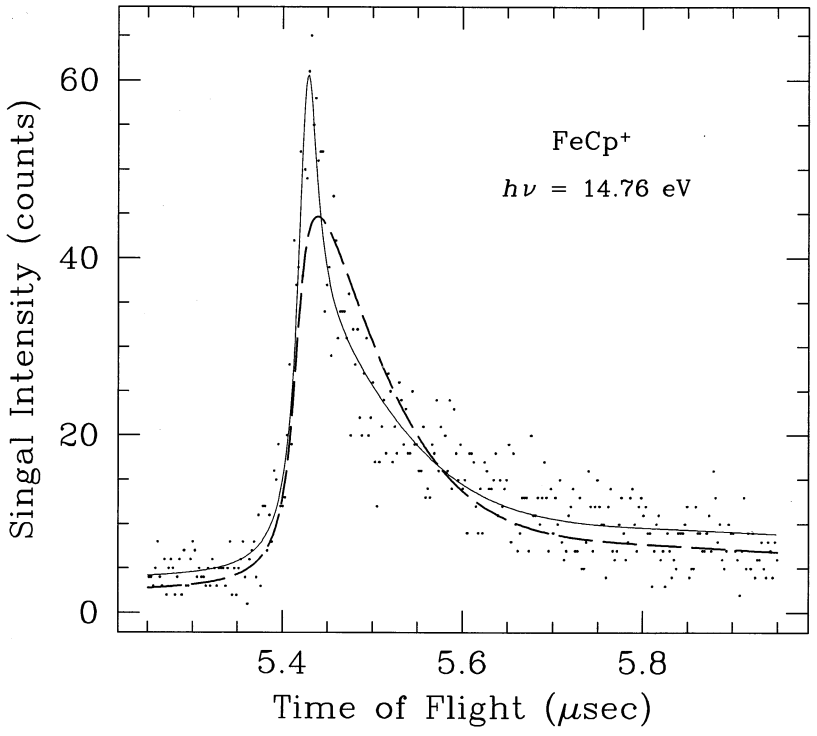

Fig. 4. The TOF shape of $Fe(C_5H_5)^+$ ion signals generated at photon energy of 14.76 eV (dotted points). The dashed line represents Eq. (3) and the solid line Eq. (4). The solid line gives a unimolecular decay constant of $k = 2.4 \pm 1.0 \times 10^6\ s^{-1}$.

of daughter ions [23]. The parent ion population in region II decays by the dissociation, following the first-order kinetics, $\exp(-kt^*)$. The value for t^* can be easily related to the experimental TOF value and the instrumental parameters such as acceleration voltage and length. The instrumental parameters have been varied in the experiment, confirming that the kinetic model used for this analysis is valid. The time range for convolution spans from the time of photoexcitation (t_0) to the time of ion escape from region II (t_f). In Fig. 4, the functional form of Eq. (3) is presented by the broken-line curve, after being optimized to the experimental TOF data. Apparently, this function fails to provide a satisfactory fit to the entire TOF distribution, particularly to the sharp peaking at the high velocity position. The sharp peaking can be reproduced only by including an additional reaction channel of rapid dissociation of parent ion, which is described by the extra Lorentzian term in Eq. (4).

$$S(t) = \sum_{t=t_0}^{t_f} \frac{A_1 e^{-kt^*}}{1 + B(t' - t)^2} + \frac{A_2}{1 + B(t_0 - t)^2} \qquad (4)$$

We use a Lorentzian form for the rapid dissociation because when the dissociation occurs within 10^{-7} s, the inherent TOF broadening, which is Lorentzian, is larger than the dissociation-induced broadening. The solid-line curve in Fig. 4 represents the best fit to the experimental data using Eq. (4). It gives $k = 2.4 \pm 1.0 \times 10^6\ s^{-1}$ for the slower dissociation channel, the uncertainty in the k value estimated from adjustment of the fitting parameters.

The measured rate of $2.4 \pm 1.0 \times 10^6\ s^{-1}$ for the dissociation reaction, $FeCp_2^{\cdot +} \rightarrow FeCp^+ + Cp^{\cdot}$, is thought to be compatible with a statistical unimolecular decay. In order to check this possibility, we compare the dissociation rate with the theoretical RRKM rate, under approximation that the absorbed photon energy is fully converted to the molecular

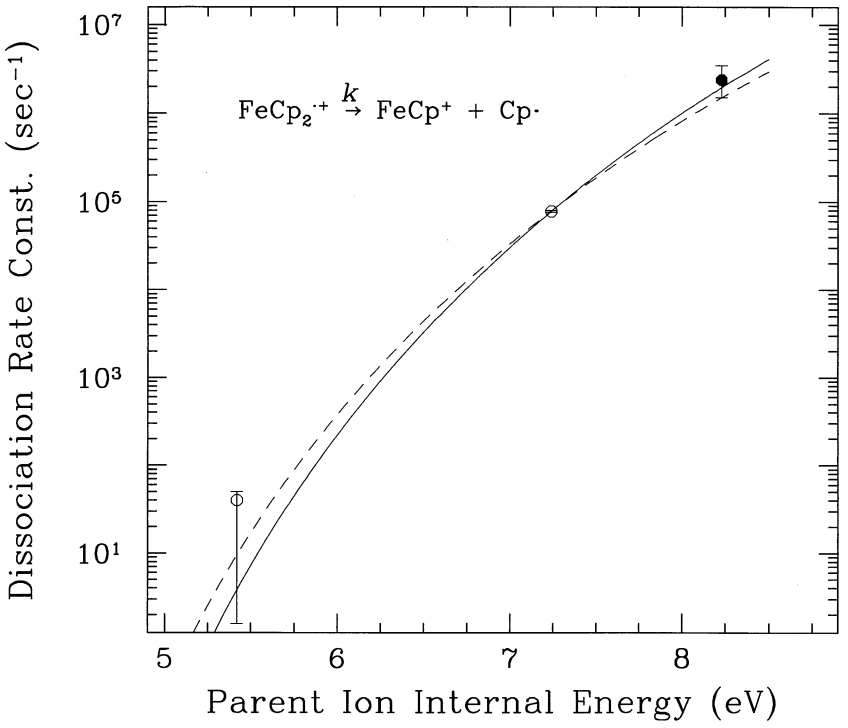

Fig. 5. The rate for dissociation reaction, $Fe(C_5H_5)_2^{\cdot+} \rightarrow Fe(C_5H_5)^+ + C_5H_5\cdot$, as a function of ion internal energy. The solid circle represents our result at photon energy of 14.76 eV, the ion internal energy being obtained by subtracting the $Fe(C_5H_5)_2$ ionization energy (6.75 eV) and adding the thermal energy (0.22 eV). The open circles are from Ref. [13]. The solid line is the RRKM curve fitted to both solid and open circles, giving $E_0 = 3.95$ eV. The dashed-line curve is from [13] with $E_0 = 3.75$ eV.

internal energy of $FeCp_2^{\cdot+}$ after the initial ionization. Such approximation is not unreasonable for the data of Fig. 4 because the photon energy of 14.76 eV is only slightly above the dissociation threshold energy (11.6–13.16 eV; Table 1), and in this case the kinetic energies of ejected electrons are probably very small. The RRKM rate has been calculated by Faulk and Dunbar [13] based on their time-resolved photodissociation study of $FeCp_2^{\cdot+}$ and using the vibrational frequencies of neutral $FeCp_2$ [9,10]. They found the most reasonable kinetic parameters to be the activation energy (E_0) of 3.40–4.05 eV and the entropy of activation (ΔS^*) of 0.90–12.66 eu. Within these parameter ranges, the RRKM curve fitted to the data of both ours and Faulk and Dunbar [13] is shown by the solid line in Fig. 5. The activation energy is 3.95 eV with $\Delta S^* = 11.39$ eu for this curve. With inclusion of the present data, the E_0 value goes toward the upper limit of the Faulk and Dunbar's value. The increase of E_0 seems to be in the right direction, considering that the data point at 5.42 eV taken from Ref. [13] gives such a margin, and that the recent electron impact study [18] has indicated a higher value for the $CpFe^+$–Cp bond dissociation energy (4.61 eV). The dashed line in the figure represents the original curve of Ref. [13], with $E_0 = 3.75$ eV and $\Delta S^* = 7.14$ eu. It is clear from this analysis that the tailing in the $FeCp^+$ peak results from slow unimolecular decay of parent $FeCp_2^{\cdot+}$ ions in region II. The sharp peaking in the distribution, on the other hand, must be assigned to an alternative dissociation reaction that occurs much faster ($k > 10^7$ s^{-1}) than a statistical reaction, and consequently, via a direct nonstatistical route. It is quite plausible that this direct channel is responsible for the fast ligand dissociation reactions ($k \geq 10^8$ s^{-1}) observed in the previous UV MPI/MPD studies [16–18].

4. Conclusion

The photoionization and photodissociation reactions of ferrocene have been investigated under the condition of VUV single photon absorption (14–33 eV). The major ionic products are $FeCp_2^{\cdot+}$, $FeCp^+$ and $Fe^{\cdot+}$, well expected from Cp· ligand dissociation. The ligand dissociation occurs largely in a sequential way, but concerted elimination of two Cp· rings is also indicated by the $C_{10}H_x^{\cdot+}$ ($x = 8$–10) production. The concerted elimination reaction is one of the features that distinguish VUV single photon excitation from UV multiphoton excitation. The concerted reaction probably involves the electronic excited states of long life-times populated by VUV absorption. The rate for CpFe–Cp dissociation has been estimated by analyzing the asymmetric TOF distribution shape of $FeCp^+$ signals. The dissociation occurs via two channels, the direct dissociation occurring inside the ionization region right after VUV excitation and the slow unimolecular decay. The unimolecular decay rate of $k = 2.4 \pm 1.0 \times 10^6\ s^{-1}$ observed at photon energy of 14.76 eV is well in accord with the calculated RRKM value. The kinetic information deduced for these channels is quantitatively valid only for low photon energies. More accurate information over a wider energy range will require further investigation based on a photoelectron photoion coincidence study using electron energy analysis.

Acknowledgements

The experiment at PLS was supported in part by MOST and POSCO. The School of Environmental Engineering and KOSEF (CMS) are acknowledged for this project. S.-J. Han thanks Korea Research Foundation for the salary support.

References

[1] Vacuum Ultraviolet Photoionization and Photodissociation of Molecules and Clusters, C.Y. Ng (Ed.), World Scientific, Singapore, 1991.
[2] VUV and Soft X-ray Photoionization, U. Becker, D.A. Shirley (Eds.), Plenum, New York, 1996.
[3] T. Baer, Annu. Rev. Phys. Chem. 40 (1989) 637.
[4] H. Koch, P. Jørgense, T. Helgaker, J. Chem. Phys. 104 (1996) 9528.
[5] W. Klopper, H.P. Lüthi, Chem. Phys. Lett. 262 (1996) 546.
[6] A.T. Armstrong, F. Smith, E. Elder, S.P. McGlynn, J. Chem. Phys. 46 (1967) 4321.
[7] Y.S. Sohn, D.N. Hendrickson, H.B. Gray, J. Am. Chem. Soc. 93 (1971) 3603.
[8] E.R. Lippincott, R.D. Nelson, J. Am. Chem. Soc. 77 (1955) 4990.
[9] E.R. Lippincott, R.D. Nelson, Spectrochim. Acta 10 (1958) 307.
[10] H.P. Fritz, Adv. Organomet. Chem. 1 (1964) 239.
[11] H.T. Liou, Y. Ono, P.C. Engelking, J.T. Moseley, J. Phys. Chem. 90 (1986) 2888; H.T. Liou, P.C. Engelking, Y. Ono, J.T. Moseley, ibid. 90 (1986) 2892.
[12] U. Ray, H.Q. Hou, Z. Zhang, W. Schwarz, M. Vernon, J. Chem. Phys. 90 (1989) 4248.
[13] J.D. Faulk, R.C. Dunbar, J. Am. Chem. Soc. 114 (1992) 8596.
[14] M. Panczel, T. Baer, Int. J. Mass Spectrom. Ion Processes 58 (1984) 43.
[15] S. Leutwyler, U. Even, J. Jortner, Chem. Phys. Lett. 74 (1980) 11.
[16] S. Niles, D.A. Prinslow, C.A. Wight, P.B. Armentrout, J. Chem. Phys. 97 (1992) 3115.
[17] J. Opitz, D. Bruch, G. von Bünau, Org. Mass Spectrom. 28 (1993) 405.
[18] J. Opitz, P. Härter, Int. J. Mass Spectrom. Ion Processes 121 (1992) 183.
[19] R. Bär, Th. Heinis, Ch. Nager, M. Jungen, Chem. Phys. Lett. 91 (1982) 440.
[20] G.D. Flesch, G.A. Junk, H.J. Svec, J. Chem. Soc. Dalton Trans. 11 (1972) 1102.
[21] J.A. Burroughs, S.B. Wainhaus, L. Hanley, J. Chem. Phys. 103 (1995) 6706.
[22a] S.A. Miller, D.E. Riederer, Jr., R.G. Cooks, W.R. Cho, H.W. Lee, H. Kang, J. Phys. Chem. 98 (1994) 245.
[22b] H. Kang, H.W. Lee, W.R. Cho, S.M. Lee, Chem. Phys. Lett., in press.
[23] S. Olesik, T. Baer, J.C. Morrow, J.J. Ridal, J. Buschek, J.L. Holmes, Org. Mass Spectrom. 24 (1989) 1008.